Germylene-β-sulfoxide Hemilabile Ligand in Coordination Chemistry

Nicolas Lentz, Cynthia Cuevas-Chávez, Sonia Mallet-Ladeira, Jean-Marc Sotiropoulos, Antoine Baceiredo, Tsuyoshi Kato, David Madec

Germylene-β-sulfoxide Hemilabile Ligand in Coordination Chemistry

Nicolas Lentz, Cynthia Cuevas-Chavez, Sonia Mallet-Ladeira, Jean-Marc Sotiropoulos, Antoine Baceiredo, Tsuyoshi Kato, David Madec

Germylene-β-sulfoxide hemilabile ligand in coordination chemistry

Nicolas Lentz,[a] Cynthia Cuevas-Chavez,[a] Sonia Mallet-Ladeira,[b] Jean-Marc Sotiropoulos,[c] Antoine Baceiredo,[a] Tsuyoshi Kato,[a] David Madec* [a]

[a] Laboratoire Hétérochimie Fondamentale et Appliquée (UMR 5069), Université de Toulouse, CNRS, 118, Route de Narbonne, 31062 Toulouse Cedex 09, France.
[b] Institut de Chimie de Toulouse (ICT, FR2599), 118, Route de Narbonne, 31062 Toulouse Cedex 09, France.
[c] IPREM, UMR 5254 UPPA/CNRS – ECP Technopole Helioparc – 2, av. Pdt P. Angot – 64053 Pau cedex 09, France.

ABSTRACT: We describe herein the synthesis of a germylene-β-sulfoxide ligand **1** and its abilities in coordination chemistry. Treatment of 1 with metal complexes [W(cod)(CO)$_4$], [Mo(nbd)(CO)$_4$] and [Ni(cod)$_2$] afforded the corresponding (**1**)-chelated metal complexes (**1**)-W(CO)$_4$ **2a**, (**1**)-Mo(CO)$_4$ **2b**, and (**1**)-Ni(cod) **4a** clearly showing a bidentate ligation of the metal by the Ge(II) and the sulfur centers. Coordination with [Ru(PPh$_3$)$_3$Cl$_2$] afforded an unprecedented bridged bis-ruthenium complex **3b**. In the case of (**1**)-Ni(cod) complex **4a**, the hemilability of bidentate ligand **1** was demonstrated by the sulfoxide substitution by a CO ligand.

INTRODUCTION

Since the first description of hemilabile ligands by Jeffrey,[1] those heteroditopic structures featuring a combination of strong and weak donor groups have become essential tools in transition-metal catalysis.[2] On the other hand, the investigation of transition-metal germylene complexes has attracted considerable interest over the past few decades.[3] Thus, it has been demonstrated that germylene ligands exhibit relatively high binding energies to transition metals and are very strong donors.[3i-l] Particularly, amidinategermylenes are currently very well-known germanium(II) species and their use as ligands in transition-metals complexes has already been extensively studied.[3m-n] However, the use of transition-metal germylenes complexes in catalysis remains sporadic, with only a few recent reports in reduction, hydrocyanation of ketones, or Sonogashira cross-coupling reaction (Figure 1).[4]

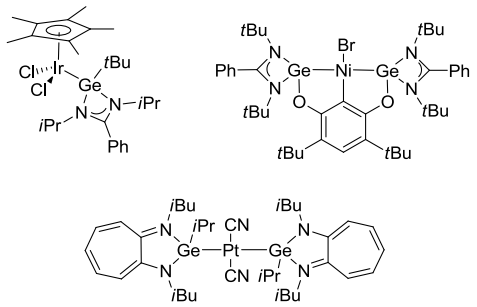

Figure 1. Examples of transition-metal germylenes used in catalysis.

In this context, we have recently reported the synthesis of germylene-α-sulfoxide as potential hemilabile ligands and the characterization of the corresponding W(0)-, Mo(0)- and Ru(II)-complexes (Figure 2).[5]

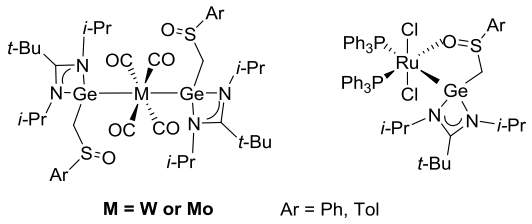

Figure 2. Mo(0)-, W(0)- and Ru(II)-complexes incorporating germylene-α-sulfoxide ligands

From these preliminary results, we envisioned to modulate their coordination properties by the skeleton design. Herein, we report the synthesis of a germylene-β-sulfoxide ligand **1**, and its bridging capability as bidentate ligand towards transition metal complexes. Furthermore, the hemilabile nature of this bidentate ligand will be explored in the case of the corresponding Ni(0)-complex.

RESULTS AND DISCUSSION

Germylene-β-sulfoxide ligand **1** was prepared by reaction of [*i*PrNC(*t*Bu)N*i*Pr]GeCl with sulfinyl carbanion. The choice of sulfoxide moiety was focused on the use of *tert*-butyl-*p*-tolyl-sulfoxide, allowing a directed ortho-metalation. The β–Sulfinyl carbanion, prepared by deprotonation of *tert*-butyl-*p*-tolyl-sulfoxide with *n*-BuLi at -80 °C in toluene solution, was added to one equivalent of [*i*PrNC(*t*Bu)N*i*Pr]GeCl, leading to β-Sulfinyl germylene **1** as an air-sensitive oil in 82% yield (Scheme 1).

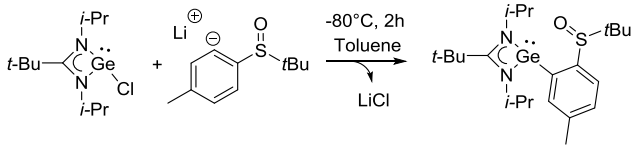

Scheme 1. Synthesis of β-sulfinyl germylene **1**.

In the solid state, at -24 °C and under inert conditions, **1** is perfectly stable, but all attempts to grow single crystals failed. Ligand **1** has been fully characterized by NMR spectroscopy, and the ^{1}H NMR spectrum exhibits a characteristic singlet at 7.65 ppm corresponding to the hydrogen in *ortho*-position relative to germylene moiety. Moreover, due to the presence of stereogenic sulfoxide center, *CH*$_3$ substituents of *i*Pr groups appear as four doublets at 0.66, 0.92, 1.09 and 1.23 ppm, ($^{3}J_{HH}$ = 6.3 Hz) and two different septuplets at 3.97 and 4.10 ppm ($^{3}J_{HH}$ = 6.3 Hz) were observed for both *CH*-protons. The ^{13}C NMR spectrum exhibits a characteristic signal at 138.8 ppm for the quaternary aromatic carbon atom bonded to Ge(II) center. Again, the chiral sulfoxide fragment induces the loss of symmetry of *i*Pr groups showing two different signals at 47.3 and 47.4 ppm for the *CH* and four singlets for the *CH*$_3$ (24.2, 24.4, 27.5 and 27.7 ppm).

The coordination ability of this new β-sulfinyl germylene ligand **1** towards transition metals was investigated with [W(cod)(CO)$_4$] (cod = 1,5-cyclooctadiene) and [Mo(nbd)(CO)$_4$] (nbd = 2,5-norbornadiene) (Scheme 2). Cyclooctadiene (cod) or norbornadiene (nbd) were easily displaced by germanium(II) species **1** in THF solution at room temperature, and complexes **2a** and **2b** were isolated as pale yellow powders in 89% and 78% yields, respectively.

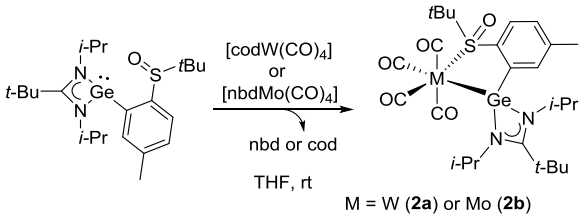

Scheme 2. Synthesis of complexes **2a** and **2b**.

Analytically pure crystals of **2a** and **2b** were obtained from THF solutions. The ^{13}C NMR spectra exhibit four characteristic signals (**2a**: 202.1, 206.7, 208.3 and 210.2 ppm; **2b**: 209.3, 214.0, 216.9 and 220.8 ppm) corresponding to the carbonyl ligands, in agreement with a bidentate ligation of the metal by **1**. Moreover, the coordination of the sulfinyl group to the transition metal was confirmed by IR spectroscopy with characteristic S=O absorptions at 1067 cm^{-1} for **2a** and 1089 cm^{-1} for **2b**.[6] In both cases, X-ray diffraction analysis clearly indicate the bidentate coordination of the tungsten and the molybdenum atoms by the germylene and the sulfur of the sulfinyl group (Figure 3).

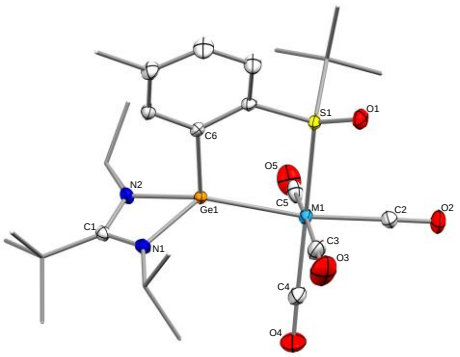

Figure 3. Molecular structures of **2a** (M1 = W) and **2b** (M1 = Mo). Thermal ellipsoids are set at 50% probability. Hydrogen atoms and solvent molecule have been omitted for clarity. Selected bond distances [Å] and bond angles [deg] for **2a**: Ge1−N1 1.952(3); Ge1−N2 1.951(3); Ge1−C6 1.970(4); C1−N1 1.341(5); C1−N2 1.330(5); Ge1−W1 2.566 (1); S1-W1 2.50 1(1); S1-O1 1.482(3); N1−Ge1−N2 66.40(12); N2−Ge1−C6 105.38(14); N1−Ge1−C6 102.09(14); N2−Ge1−W1 137.31(9); N1−Ge1−W1 131.23(9); C6-Ge1-W1 106.61(10). Selected bond distances [Å] and bond angles [deg] for **2b**: Ge1−N1 1.955(3); Ge1−N2 1.969(2); Ge1−C6 1.975(2); C1−N1 1.343(3); C1−N2 1.340(3); Ge1−Mo1 2.563(1); S1-Mo1 2.521 (1); S1-O1 1.490(2); N1−Ge1−N2 66.33(8); N2−Ge1−C6 103.06(9); N1−Ge1−C6 101.60(9); N2−Ge1−Mo1 139.83(6); N1−Ge1−Mo1 130.67(6); C6−Ge1−Mo1 106.75(7).

The asymmetric unit for **2a** and **2b** each contains two independent molecules with similar metrical data and the discussion is restricted to one of them. In both molecular structures the germanium atom adopts a distorted tetrahedral geometry, and the transition metals (W or Mo) are octahedrally coordinated with a classical W−Ge bond distance of 2.566(1) Å,[7a-d] and a slightly elongated Mo−Ge of 2.563(1) Å.[7a, 7f-g] Ge1−N1 and Ge1−N2 bond lengths [**2a**:1.951(3) and 1.952(3) Å; **2b**:1.955(2) and 1.969(2) Å] are equal and shorter than in the starting chloro-germylene (1.98 Å). It is important to note that **2a** and **2b** are, to the best of our knowledge, the first examples of crystallized W(0) and Mo(0) complexes coordinated by the sulfur atom of a sulfoxide function.

In the continuity of our study we have investigated the reactivity of ligand **1** with a Ru(II)-complex. Therefore, a THF solution of an equimolar amount of [Ru(PPh$_3$)$_3$Cl$_2$] and **1** was stirred overnight at room temperature (Scheme 3).

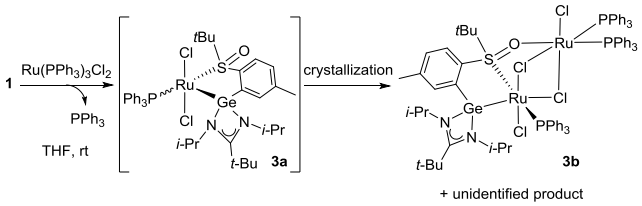

Scheme 3. Synthesis of complex **3a** and **3b**.

The reaction can be easily monitored by ^{31}P NMR spectroscopy which shows the clean formation of a new complex whose structure is potentially compatible with **3a**, with a sin-

glet at 38 ppm, and a signal at -5 ppm corresponding to the free Ph_3P. Moreover, the sulfur-coordination was assumed by IR spectroscopy with a characteristic band at 1095 cm^{-1}. Although **3a** was identified by HRMS analysis, all crystallization attempts afforded systematically the bis-ruthenium complex **3b**. Multi nuclear NMR of **3b** in CD_2Cl_2 showed the presence of three isomers in solution (see SI). Considering modelisation using DFT (slightly simplified by using an ethylenic group instead of the aryl linker between the sulfur and germanium atoms) we found three ligand position isomers exist on this surface. They correspond to different positions of the chlorine atoms and phosphine moiety (see SI). However, these isomers are very similar in energy (between 4 and 7 kcal/mol) and probably coexist in solution.

The molecular structure of **3b** exhibits two slightly distorted octahedral geometries around ruthenium atoms with chlorine and sulfoxide bridges (Figure 4). The Ge-Ru bond distance of 2.367(1) Å is in the range of already reported complexes (2.28-2.50 Å).[4e,8] Due to the bridge structure, the bond angles involving axial chlorine atoms are quite distorted: Cl1−Ru1−Cl2 of 170.41(3)° and Cl4−Ru2−Cl2 of 159.53(3)°. Ge1−Ru1−S1 and Ge1−Ru1−P1 bond angles of the 5-member ring are 84.34(3)° and 96.50(3)° respectively. The Ru−O distance [2.196(2) Å] is in the range of reported complexes bearing a phosphine in trans position (2.15-2.24 Å),[9] but it is slightly longer than in the μ–SO bridge of complexes already reported (2.06-2.16 Å).[10] Finally, the Ru−S bond length of 2.337 (1) Å is in the top range of bridge μ–SO complexes already described (2.19-2.34 Å),[10a-c] probably due to the trans-influence of phosphine ligand. It is important to note that even though μ–SO bridged binuclear transition metal complexes were already observed in the literature with ruthenium and rhodium,[10] all the complexes characterized were obtained with DMSO and **3b** is therefore the first example of μ–SO bridged ruthenium complex with an asymmetric sulfoxide. Furthermore, to the best of our knowledge, **3b** is the first crystallographically characterized complex featuring two bridge chlorine atoms, and a trans-phosphine-sulfoxide arrangement.

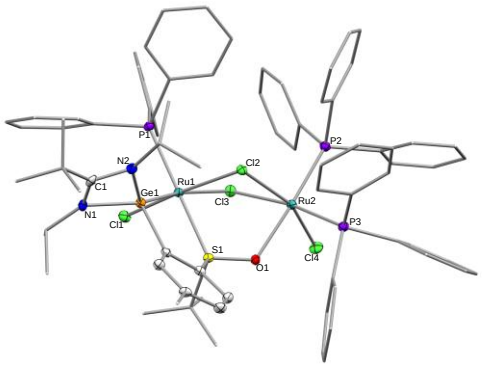

Figure 4. Molecular structure of **3b**. Thermal ellipsoids are set at 50% probability. Hydrogen atoms and solvent molecule have been omitted for clarity. Selected bond distances [Å] and bond angles [deg]: Ge1−N1 1.966(3); Ge1−N2 1.969(3); Ge1−C12 1.978(4); Ge1−Ru1 2.367(1); S1−O1 1.514(2); Ru1−P1 2.367(1); Ru2−P2 2.274(1); Ru2−P3 2.307(2); Ru1−Cl1 2.402(1); Ru1−Cl2 2.456(1); Ru1−Cl3 2.449(1); Ru2−Cl4 2.378(1); Ru2−Cl2 2.485(1); Ru2−Cl3 2.472(1); S1−Ru1 2.337(1); Ru2−O1 2.196(2); N1−Ge1−N2 66.25(12); N1−Ge1−C12 101.20(14); N2−Ge1−C12 97.48(14); N1−Ge1−Ru1 141.67(9); N2−Ge1−Ru1 133.90(9); Ge1−Ru1−P1 96.50(3); Ge1−Ru1−S1 84.34(3); P2-Ru2-P3 97.15(4); O1-Ru2-P2 175.85(7); O1-Ru2-P3 86.99(7).

$[Ni(cod)_2]$ also readily reacts with an equimolar amount of **1** in toluene solution at room temperature, to give Ni(0)-complex **4a** as a very unstable yellow solid (Scheme 4). Complex **4a** has been characterized by ^1H NMR spectroscopy, and yellow crystals, suitable for an X-ray diffraction analysis, were obtained from a -24°C toluene cold solution.

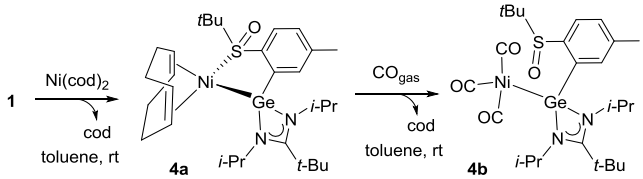

Scheme 4. Synthesis of Ni(0)-complexes **4a** and **4b**.

The molecular structure of **4a** (Figure 5) exhibits a distorted tetrahedral geometry around germanium center with a Ge1−Ni1 bond length of 2.263(1) Å in the range of already reported for Ge(II) −Ni(0)-complexes (2.09-2.30 Å).[4c,7g,11] The Ni1−S1 bond distance [2.159(1) Å] is slightly longer in comparison of the results already published (2.10-2.13 Å).[12] Within the five membered ring the Ge1−Ni1−S1 bond angle is 90.03(2)°, and it is important to note that Ge1−N1 and Ge1−N2 bond lengths [1.991(2) and 1.989(2) Å] are in the same range than the free chloro-germylene (1.98 Å). Indeed, upon coordination of an amidinato-germylene to a transition metal, usually the Ge-N bond lengths decrease due to a stronger p-donation of nitrogen to germanium. In the case of complex **4a**, this interaction is probably attenuated due to the presence of an electron rich Ni(0)-center and therefore an important π–back donation to the germylene center.

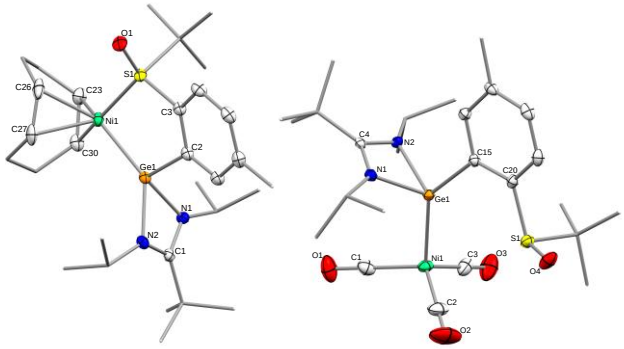

Figure 5. Molecular structure of **4a** and **4b**. Thermal ellipsoids are set at 50% probability. Hydrogen atoms have been omitted for clarity. Selected bond distances [Å] and bond angles [deg] for **4a**: Ge1−N1 1.991(2); Ge1−N2 1.989(2); Ge1−C2 1.986(2); Ge1−Ni1 2.263(1); S1−O1 1.498(2); S1-Ni1 2.159(1); Ni1−C30 2.077(2); Ni1−C26 2.096(2); Ni1−C23 2.112(2); Ni1−C27 2.134(2); N1−Ge1−N2 65.41(5); N1−Ge1−C2 104.11(6); N2−Ge1−C2 101.28(6); N1−Ge1−Ni1 134.13(4); N2−Ge1−Ni1 139.97(4);

Ge1−Ni1−S1 90.03(2). Selected bond distances [Å] and bond angles [deg] for **4b**: Ge1−N1 1.970(2); Ge1−N2 1.961(2); Ge1−C15 2.007(2); Ge1−Ni1 2.320(1); S1−O4 1.495(2); N1−Ge1−N2 66.03(7); N1−Ge1−C15 97.82(8); N2−Ge1−C15 100.22(8); N1−Ge1−Ni1 116.01(6); N2−Ge1−Ni1 116.40(5).

Interestingly, under pressure of carbon monoxide (1.0 bars), **4a** undergoes a fast ligand exchange reaction at room temperature in toluene solution, leading to the stable tricarbonyl Ni(0)-complex **4b** (Scheme 4). The substitution of the weak σ–donor sulfinyl moiety by a CO ligand clearly demonstrates the hemilabile character of the new β−sulfinyl germylene ligand **1**. Complex **4b** has been fully characterized by NMR (particularly, only one signal was observed at 199 ppm for the three CO-ligands in the ^{13}C NMR spectrum), and by IR spectroscopy with a band at 1027 cm^{-1} confirming the absence of any interaction between sulfoxide and nickel. Finally, single crystals of **4b** were obtained from a saturated toluene solution at -24 °C, and its structure was confirmed by an X-ray diffraction analysis (Figure 4). The molecular structure of **4b** exhibits a tetrahedral geometry at the nickel center with a slightly longer Ge1−Ni1 bond length of 2.320(1) Å, but still in the range of already reported germylene-nickel complexes (2.09-2.30 Å).11 Ge1-N1 and Ge1−N2 bond lengths of 1.970(2) and 1.961(2) Å are equal and shorter than in the free AmGeCl (1.98 Å), suggesting that Ni→Ge π-backbonding decreases in **4b** than in **4a**. The IR spectrum of **2a** shows a ν_{CO} (A1) stretching frequency at 2058 cm^{-1} which is shifted to lower wavenumbers in comparison to the related $Me_3P\text{-}Ni^0(CO)_3$ complex (2066 cm^{-1}), and to higher values compare to $NHC\text{-}Ni^0(CO)_3$ (IMes, 2052 cm^{-1}).[13] Therefore, the electron-donating character of germylene ligand in **4a** stands between the σ–donation strength of trialkylphosphines and N-heterocyclic carbenes (NHCs).

CONCLUSION

In conclusion, we have described the synthesis of a new β-sulfinyl germylene ligand **1** and its application in coordination chemistry. Of particular interest, its bidentate nature, involving Ge(II) and sulfoxide moieties, has been clearly established by the bidentate coordination of tungsten and molybdenum atoms in the case of complexes **2a-b**. These results highlight the importance of the linker between germylene and sulfoxide entities, since the related germylene-β-sulfoxide derivatives hardly behave as bidentate ligands. The reaction of ligand **1** with $[Ru(PPh_3)_3Cl_2]$ afforded a 16-electron complex **3a**, which readily evolves during crystallization to an unprecedented bis-ruthenium complex **3b**. As expected, with $[Ni(cod)_2]$ the corresponding Ni(0)-complex **4a** with a bidentate ligation of the metal by **1** was obtained. In this case, the hemilabile character of **1** was clearly established by reaction with carbon monoxide affording a stable tricarbonyl Ni(0)-complex **4b**. Application of this new germylene-β-sulfoxide ligand in enantioselective catalysis is under investigation.

EXPERIMENTAL SECTION

General Remarks. All manipulations with air-sensitive materials were performed in a dry and oxygen-free atmosphere of argon by using standard Schlenk-line and glovebox techniques. Solvents were purified with the MBraun SBS-800 purification system. NMR spectra were recorded with the following spectrometers: ^1H, Bruker Avance II 300 (300.18 MHz) and Avance III HD 500 MHz; ^{13}C, Bruker Avance II 300 (75.48 MHz) and Avance III HD 500 MHz; ^{31}P, Bruker Avance II 300 (75.48 MHz) and Avance III HD 500 MHz at 298 K. Mass spectra were measured on a direct chemical ionization (DCI-CH4) methods, and recorded on a GCT Premier Waters mass spectrometer

Melting points were measured with a capillary electrothermal apparatus. IR spectra were measured on a Varian 640-IR FT-IR spectrometer. [*i*PrNC(tBu)N*i*Pr]GeCl was prepared according to literature procedures.[3-l] All reagents were obtained from commercial suppliers unless otherwise statement.

Single-crystal X-ray data were collected at low temperature (193(2)K) on a Bruker-AXS APEX II Quazar diffractometer equipped with a 30W air-cooled microfocus source (**3b** and **4b**) or on a Bruker-AXS PHOTON100 D8 VENTURE diffractometer (**2a**, **2b** and **4a**), using MoK_α radiation (λ= 0.71037 Å). The structures were solved by intrinsic phasing method (SHELXT)[14] and refined by full-matrix least-squares method on F2.[15] All non-H atoms were refined with anisotropic displacement parameters.

For **3b**, some solvent molecules were highly disordered and difficult to model correctly. Therefore, the SQUEEZE function of PLATON[16] was used to eliminate the contribution of the electron density of those solvent molecules from the intensity data.

DFT calculations have been carried out with the B3LYP functional as implemented in Gaussian 09.[17] Ru atom was described with the relativistic electron core potential SDD and the associated basis set.[18] They have been augmented by a set of f polarization functions.[19] The 6-31G** basis set was employed for all other atoms. Full optimizations for all minima structures were performed. Frequency calculations were undertaken at the same level of theory than optimization to confirm the nature of the stationary points, yielding zero imaginary frequency.

Synthesis of 1: *n*-BuLi (0.72 mmol, 0.48 mL, C = 1.6 mol/L in hexane, 1.1 eq) was added dropwise to a solution of *t*-butyl-*p*-tolylsulfoxide (141.1 mg, 0.72 mmol, 1.1 eq) in toluene (3 mL) at -78 °C. The solution was stirred during 1 hour at the same temperature (-78 °C). Then the mixture was added dropwise to a solution of AmGeCl (189 mg, 0.65 mmol, 1 eq) in toluene (3 mL) at -78 °C. The mixture was stirred during 2 hours at -78 °C and then warmed up to room temperature slowly. The solvent was evaporated under reduced pressure, the crude was then extracted with toluene (2x 2mL) and concentrated in order to afford a yellow oil (241 mg) in 82% yield. The compound is stable and storable at -24 °C in an inert atmosphere of argon. ^1H NMR (300.18 MHz, C_6D_6, 25 °C): δ 0.66 (d, $^3J_{HH}$ = 6.3 Hz, 3H, $CH(C\boldsymbol{H}_3)_2$); 0.92 (d, $^3J_{HH}$ = 6.3 Hz, 3H, $CH(C\boldsymbol{H}_3)_2$); 1.09 (d, $^3J_{HH}$ = 6.3 Hz, 3H, $CH(C\boldsymbol{H}_3)_2$); 1.14 (s, 9H, $C(C\boldsymbol{H}_3)_3$); 1.23 (d, $^3J_{HH}$ = 6.3 Hz, 3H, $CH(C\boldsymbol{H}_3)_2$); 1.29 (s, 9H, $C(C\boldsymbol{H}_3)_3$); 2.20 (s, 3H, *p*-$C\boldsymbol{H}_3$); 3,97 (sept., $^3J_{HH}$ = 6.3 Hz, 1H, $C\boldsymbol{H}(CH_3)_2$); 4.10 (sept., $^3J_{HH}$ = 6.3 Hz, 1H, $C\boldsymbol{H}(CH_3)_2$); 7.04 (d, 1H, $^3J_{HH}$ = 8.2 Hz, $C\boldsymbol{H}_{Ar}$); 7.64 (s,

1H, C$\boldsymbol{H}_{Ar}$); 7.97 (d, 1H, $^{3}J_{HH}$ = 8.2 Hz, C$\boldsymbol{H}_{Ar}$). $^{13}C\{^{1}H\}$ NMR (75.48 MHz, C_6D_6, 25 °C): δ 21.5 (*p*-C$\boldsymbol{H}_3$); 23.8 (O=SC($\boldsymbol{C}H_3$)$_3$); 24.2 (CH($\boldsymbol{C}H_3$)$_2$); 24.4 (CH($\boldsymbol{C}H_3$)$_2$); 27.5 (CH($\boldsymbol{C}H_3$)$_2$); 27.7 (CH($\boldsymbol{C}H_3$)$_2$); 29.3 (C($\boldsymbol{C}H_3$)$_3$); 40.2 ($\boldsymbol{C}$(CH$_3$)$_3$); 47.3 ($\boldsymbol{C}$H(CH$_3$)$_2$); 47.4 ($\boldsymbol{C}$H(CH$_3$)$_2$); 56.5 (O=S-$\boldsymbol{C}$(CH$_3$)$_3$); 125.9 ($\boldsymbol{C}_{Ar}$); 128.8 ($\boldsymbol{C}_{Ar}$); 132.6 ($\boldsymbol{C}_{Ar}$); 138.8 ($\boldsymbol{C}_{Ar/q}$); 145.8 ($\boldsymbol{C}_{Ar/q}$); 159.5 ($\boldsymbol{C}_{Ar/q}$); 171.9 (N−$\boldsymbol{C}$−N).

Synthesis of 2a: 1 (140 mg, 0.31 mmol, 1 eq) was dissolved in THF (3 mL) and added to tetracarbonyl(1,5-cyclooctadiene) tungsten (0) (125 mg, 0.31 mmol, 1 eq) in THF (1 mL). The mixture was stirred during 15 hours at room temperature, then filtered and the solvent removed under reduced pressure. Finally, the solid was washed with pentane (2 x 3 mL) to obtain a pale yellow solid (206 mg) in 89% yield. Crystallization from a solution of THF at 6 °C gave pale yellow crystals suitable for X-ray diffraction analysis. M.p. : 117 °C (decomposition); ^{1}H NMR (300.18 MHz, C_6D_6, 25 °C): δ 0.54 (d, $^{3}J_{HH}$ = 6.3 Hz, 3H, CH(C$\boldsymbol{H}_3$)$_2$); 0.81 (d, $^{3}J_{HH}$ = 6.3 Hz, 3H, CH(C$\boldsymbol{H}_3$)$_2$); 1.06 (s, 9H, C(C$\boldsymbol{H}_3$)$_3$); 1.20 (s, 9H, C(C$\boldsymbol{H}_3$)$_3$); 1.23 (d, $^{3}J_{HH}$ = 6.3 Hz, 3H, CH(C$\boldsymbol{H}_3$)$_2$); 1.29 (d, $^{3}J_{HH}$ = 6.3 Hz, 3H, CH(C$\boldsymbol{H}_3$)$_2$); 2.13 (s, 3H, *p*-C$\boldsymbol{H}_3$); 3.98 (sept., $^{3}J_{HH}$ = 6.3 Hz, 1H, C$\boldsymbol{H}$(CH$_3$)$_2$); 4.08 (sept., $^{3}J_{HH}$ = 6.3 Hz, 1H, C$\boldsymbol{H}$(CH$_3$)$_2$); 6.87 (d, 1H, $^{3}J_{HH}$ = 8.2 Hz, C$\boldsymbol{H}_{Ar}$); 7.34 (s, 1H, C$\boldsymbol{H}_{Ar}$); 8.17 (d, 1H, $^{3}J_{HH}$ = 8.2 Hz, C$\boldsymbol{H}_{Ar}$). $^{13}C\{^{1}H\}$ NMR (75.48 MHz, C_6D_6, 25 °C): δ 20.9 (p-$\boldsymbol{C}H_3$); 22.9 (CH($\boldsymbol{C}H_3$)$_2$); 24.0 (O=SC($\boldsymbol{C}H_3$)$_3$); 24.8 (CH($\boldsymbol{C}H_3$)$_2$); 25.6 (CH($\boldsymbol{C}H_3$)$_2$); 25.7 (CH($\boldsymbol{C}H_3$)$_2$); 29.2 (C($\boldsymbol{C}H_3$)$_3$); 39.9 ($\boldsymbol{C}$(CH$_3$)$_3$); 47.3 ($\boldsymbol{C}$H(CH$_3$)$_2$); 48.1 ($\boldsymbol{C}$H(CH$_3$)$_2$); 65.8 (O=S-$\boldsymbol{C}$(CH$_3$)$_3$); 125.7 ($\boldsymbol{C}_{Ar}$); 130.0 ($\boldsymbol{C}_{Ar}$); 130.1 ($\boldsymbol{C}_{Ar}$); 140.9 ($\boldsymbol{C}_{Ar/q}$); 149.4 ($\boldsymbol{C}_{Ar/q}$); 153.4 ($\boldsymbol{C}_{Ar/q}$); 177.9 (N−$\boldsymbol{C}$−N); 202.1 ($\boldsymbol{C}$O); 206.7 ($\boldsymbol{C}$O); 208.3 ($\boldsymbol{C}$O); 210.2 ($\boldsymbol{C}$O). IR (Nujol, cm^{-1}) : 2012 (s) (CO), 1901 (br) (CO), 1067 (s) (SO). MS m/z (%): 704.1 ([M – (CO+CH$_3$)]$^+$). HRMS m/z (%): 747.1320 ([M + 1]$^+$) calcd for $C_{26}H_{38}GeN_2O_5WS$ ([M + 1]$^+$) 747.1311.

Synthesis of 2b: 1 (100 mg, 0.22 mmol, 1 eq) was dissolved in THF (3 mL) and added to tetracarbonyl(bicyclo[2.2.1]hepta-2,5-diene) molybdenum (0) (66 mg, 0.22 mmol, 1 eq) in THF (1 mL). The mixture was stirred during 15 hours at room temperature, then filtered and the solvent removed under reduced pressure. Finally, the solid was washed with pentane (2 x 3 mL) to obtain a pale yellow solid (113 mg) in 78% yield. Crystallization from a solution of THF at 6 °C gave pale yellow crystals suitable for X-ray diffraction analysis. M.p. : 98 °C (decomposition); ^{1}H NMR (300.18 MHz, C_6D_6, 25 °C): δ 0.54 (d, $^{3}J_{HH}$ = 6.3 Hz, 3H, CH(C$\boldsymbol{H}_3$)$_2$); 0.80 (d, $^{3}J_{HH}$ = 6.3 Hz, 3H, CH(C$\boldsymbol{H}_3$)$_2$); 1.05 (s, 9H, C(C$\boldsymbol{H}_3$)$_3$); 1.20 (s, 9H, C(C$\boldsymbol{H}_3$)$_3$); 1.22 (d, $^{3}J_{HH}$ = 6.3 Hz, 3H, CH(C$\boldsymbol{H}_3$)$_2$); 1.29 (d, $^{3}J_{HH}$ = 6.3 Hz, 3H, CH(C$\boldsymbol{H}_3$)$_2$); 2.11 (s, 3H, *p*-C$\boldsymbol{H}_3$); 3.91 (sept., $^{3}J_{HH}$ = 6.3 Hz, 1H, C$\boldsymbol{H}$(CH$_3$)$_2$); 4.03 (sept., $^{3}J_{HH}$ = 6.3 Hz, 1H, C$\boldsymbol{H}$(CH$_3$)$_2$); 6.90 (d, 1H, $^{3}J_{HH}$ = 8.2 Hz, C$\boldsymbol{H}_{Ar}$); 7.32 (s, 1H, C$\boldsymbol{H}_{Ar}$); 8.14 (d, 1H, $^{3}J_{HH}$ = 8.2 Hz, C$\boldsymbol{H}_{Ar}$). $^{13}C\{^{1}H\}$ NMR (75.48 MHz, C_6D_6, 25 °C): δ 21.0 (p-$\boldsymbol{C}H_3$); 23.0 (CH($\boldsymbol{C}H_3$)$_2$); 23.9 (O=SC($\boldsymbol{C}H_3$)$_3$); 24.8 (CH($\boldsymbol{C}H_3$)$_2$); 25.8 (CH($\boldsymbol{C}H_3$)$_2$); 25.9 (CH($\boldsymbol{C}H_3$)$_2$); 29.2 (C($\boldsymbol{C}H_3$)$_3$); 39.8 ($\boldsymbol{C}$(CH$_3$)$_3$); 47.4 ($\boldsymbol{C}$H(CH$_3$)$_2$); 48.2 ($\boldsymbol{C}$H(CH$_3$)$_2$); 64.1 (O=S-$\boldsymbol{C}$(CH$_3$)$_3$); 126.1 ($\boldsymbol{C}_{Ar}$); 129.8 ($\boldsymbol{C}_{Ar}$); 130.2 ($\boldsymbol{C}_{Ar}$); 140.4 ($\boldsymbol{C}_{Ar/q}$); 148.6 ($\boldsymbol{C}_{Ar/q}$); 152.2 ($\boldsymbol{C}_{Ar/q}$); 177.3 (N−$\boldsymbol{C}$−N); 209.3 ($\boldsymbol{C}$O); 213.9 ($\boldsymbol{C}$O); 216.9 ($\boldsymbol{C}$O); 220.8 ($\boldsymbol{C}$O). IR (CH_2Cl_2, cm^{-1}) : 2005 (s) (CO), 1882 (br) (CO), 1089 (s) (SO). MS m/z (%): 659.24 ([M$^+$).

Synthesis of 3a: 1 (100 mg, 0.22 mmol, 1 eq) was dissolved in THF (3 mL) and added to tris(triphenylphosphine) ruthenium dichloride (211 mg, 0.22 mmol, 1 eq). The mixture was stirred during 15 hours at room temperature, then filtered and the solvent removed under reduced pressure. Finally, the crude was dissolved in THF (2 mL) and pentane (8 mL) was added slowly to precipitate **3a**. After filtration and drying, a red solid (135 mg) in 69% yield was obtained with 15% of PPh_3 remaining. $^{31}P\{^{1}H\}$ NMR (121.49 MHz, C_6D_6): δ 38.0 (s, Ru-*P*Ph$_3$). HRMS m/z (%): 850.1379 ([M + ACN – Cl – ^{i}Pr]$^+$) calcd for $C_{39}H_{49}ClGeN_3OPRuS$ ([M + ACN – Cl – ^{i}Pr]$^+$) 850.1368, 809.1114 ([M – Cl – ^{i}Pr]$^+$), 809.1114 ([M – Cl – ^{i}Pr]$^+$) calcd for $C_{37}H_{47}ClGeN_2OPRuS$ ([M + ACN – Cl – ^{i}Pr]$^+$) 809.1102. IR (CH_2Cl_2, cm^{-1}) : 1095 (s) (SO).

Synthesis of 3b: 3a (135 mg, 0.15 mmol, 1 eq) was dissolved in THF (3 mL) in a vial and pentane was added in another vial. After two days of slow diffusion of pentane into THF, the crystals were filtered and washed with THF (2x 1mL) to obtain a pink solid (42 mg). M.p. : 144 °C (decomposition); Isomer A : ^{1}H NMR (500 MHz, $CDCl_3$, 25 °C): δ 0.24 (d, $^{3}J_{HH}$ = 6.6 Hz, 3H, CH(C$\boldsymbol{H}_3$)$_2$); 0.45 (d, $^{3}J_{HH}$ = 6.6 Hz, 3H, CH(C$\boldsymbol{H}_3$)$_2$); 0.51 (d, $^{3}J_{HH}$ = 6.3 Hz, 3H, CH(C$\boldsymbol{H}_3$)$_2$); 0.81 (d, $^{3}J_{HH}$ = 6.3 Hz, 3H, CH(C$\boldsymbol{H}_3$)$_2$); 1.52 (s, 9H, C(C$\boldsymbol{H}_3$)$_3$); 1.59 (s, 9H, C(C$\boldsymbol{H}_3$)$_3$); 2.42 (s, 3H, *p*-C$\boldsymbol{H}_3$); 3.91 (sept., $^{3}J_{HH}$ = 6.3 Hz, 1H, C$\boldsymbol{H}$(CH$_3$)$_2$); 4.07 (sept., $^{3}J_{HH}$ = 6.3 Hz, 1H, C$\boldsymbol{H}$(CH$_3$)$_2$); 6.18 (d, 1H, $^{3}J_{HH}$ = 8.2 Hz, C$\boldsymbol{H}_{Ar}$); 6.72-7.43 (m, 45H, C$\boldsymbol{H}_{Ar}$); 7.91-7.94 (m, 2H, C$\boldsymbol{H}_{Ar}$). $^{13}C\{^{1}H\}$ NMR (125 MHz, $CDCl_3$, 25 °C): δ 21.5 (p-$\boldsymbol{C}H_3$); 24.4 (CH($\boldsymbol{C}H_3$)$_2$); 24.8 (CH($\boldsymbol{C}H_3$)$_2$); 25.6 (CH($\boldsymbol{C}H_3$)$_2$); 26.1 (O=SC($\boldsymbol{C}H_3$)$_3$); 27.6 (CH($\boldsymbol{C}H_3$)$_2$); 30.4 (C($\boldsymbol{C}H_3$)$_3$); 40.0 ($\boldsymbol{C}$(CH$_3$)$_3$); 46.3 ($\boldsymbol{C}$H(CH$_3$)$_2$); 48.1 ($\boldsymbol{C}$H(CH$_3$)$_2$); 71.8 (O=S-$\boldsymbol{C}$(CH$_3$)$_3$); 178.3 (N−$\boldsymbol{C}$−N). $^{31}P\{^{1}H\}$ NMR (200 MHz, C_6D_6): δ 28.7 (s, Ru-*P*Ph$_3$), 44.8 (d, $^{2}J_{PP}$ = 42.0 Hz, Ru-*P*Ph$_3$), 53.6 (d, $^{2}J_{PP}$ = 42.0 Hz, Ru-*P*Ph$_3$). Isomer B : ^{1}H NMR (500 MHz, $CDCl_3$, 25 °C): δ -0.24 (d, $^{3}J_{HH}$ = 6.6 Hz, 3H, CH(C$\boldsymbol{H}_3$)$_2$); 0.06 (d, $^{3}J_{HH}$ = 6.6 Hz, 3H, CH(C$\boldsymbol{H}_3$)$_2$); 0.23 (d, $^{3}J_{HH}$ = 6.3 Hz, 3H, CH(C$\boldsymbol{H}_3$)$_2$); 0.69 (d, $^{3}J_{HH}$ = 6.3 Hz, 3H, CH(C$\boldsymbol{H}_3$)$_2$); 1.56 (s, 9H, C(C$\boldsymbol{H}_3$)$_3$); 1.63 (s, 9H, C(C$\boldsymbol{H}_3$)$_3$); 2.45 (s, 3H, *p*-C$\boldsymbol{H}_3$); 3.77 (sept., $^{3}J_{HH}$ = 6.3 Hz, 1H, C$\boldsymbol{H}$(CH$_3$)$_2$); 3.96 (sept., $^{3}J_{HH}$ = 6.3 Hz, 1H, C$\boldsymbol{H}$(CH$_3$)$_2$); 6.72-7.43 (m, 50H, C$\boldsymbol{H}_{Ar}$). $^{13}C\{^{1}H\}$ NMR (125 MHz, $CDCl_3$, 25 °C): δ 21.5 (p-$\boldsymbol{C}H_3$); 23.5 (CH($\boldsymbol{C}H_3$)$_2$); 23.8 (CH($\boldsymbol{C}H_3$)$_2$); 25.0 (CH($\boldsymbol{C}H_3$)$_2$); 26.1 (O=SC($\boldsymbol{C}H_3$)$_3$); 26.7 (CH($\boldsymbol{C}H_3$)$_2$); 30.3 (C($\boldsymbol{C}H_3$)$_3$); 39.9 ($\boldsymbol{C}$(CH$_3$)$_3$); 47.0 ($\boldsymbol{C}$H(CH$_3$)$_2$); 48.6 ($\boldsymbol{C}$H(CH$_3$)$_2$); 71.9 (O=S-$\boldsymbol{C}$(CH$_3$)$_3$); 178.0 (N−$\boldsymbol{C}$−N). $^{31}P\{^{1}H\}$ NMR (200 MHz, C_6D_6): δ 39.9 (s, Ru-*P*Ph$_3$), 41.6 (d, $^{2}J_{PP}$ = 37.3 Hz, Ru-*P*Ph$_3$), 44.1 (d, $^{2}J_{PP}$ = 37.3 Hz, Ru-*P*Ph$_3$). Isomer C : ^{1}H NMR (500 MHz, $CDCl_3$, 25 °C): δ 0.00 (d, $^{3}J_{HH}$ = 6.6 Hz, 3H, CH(C$\boldsymbol{H}_3$)$_2$); 0.16 (d, $^{3}J_{HH}$ = 6.6 Hz, 3H, CH(C$\boldsymbol{H}_3$)$_2$); 0.39 (d, $^{3}J_{HH}$ = 6.3 Hz, 3H, CH(C$\boldsymbol{H}_3$)$_2$); 0.98 (d, $^{3}J_{HH}$ = 6.3 Hz, 3H, CH(C$\boldsymbol{H}_3$)$_2$); 1.52 (s, 9H, C(C$\boldsymbol{H}_3$)$_3$); 1.59 (s, 9H, C(C$\boldsymbol{H}_3$)$_3$); 2.46 (s, 3H, *p*-C$\boldsymbol{H}_3$); 3.79 (sept., $^{3}J_{HH}$ = 6.3 Hz, 1H, C$\boldsymbol{H}$(CH$_3$)$_2$); 4.04 (sept., $^{3}J_{HH}$ = 6.3 Hz, 1H, C$\boldsymbol{H}$(CH$_3$)$_2$); 6.72-7.43 (m, 49H, C$\boldsymbol{H}_{Ar}$); 8.44 (d, 1H, $^{3}J_{HH}$ = 8.2 Hz, C$\boldsymbol{H}_{Ar}$). $^{13}C\{^{1}H\}$ NMR (125 MHz, $CDCl_3$, 25 °C): δ 21.7 (p-$\boldsymbol{C}H_3$); 23.2 (CH($\boldsymbol{C}H_3$)$_2$); 24.3 (CH($\boldsymbol{C}H_3$)$_2$); 24.5 (CH($\boldsymbol{C}H_3$)$_2$; 26.1 (O=SC($\boldsymbol{C}H_3$)$_3$); 27.7 (CH($\boldsymbol{C}H_3$)$_2$); 30.2 (C($\boldsymbol{C}H_3$)$_3$); 40.1 ($\boldsymbol{C}$(CH$_3$)$_3$); 46.5 ($\boldsymbol{C}$H(CH$_3$)$_2$); 48.6 ($\boldsymbol{C}$H(CH$_3$)$_2$); 69.7 (O=S-$\boldsymbol{C}$(CH$_3$)$_3$); 178.4 (N−$\boldsymbol{C}$−N). $^{31}P\{^{1}H\}$ NMR (200 MHz, C_6D_6): δ 29.5 (s, Ru-*P*Ph$_3$), 47.6 (d, $^{2}J_{PP}$ = 40.9 Hz, Ru-*P*Ph$_3$), 48.3 (d, $^{2}J_{PP}$ = 40.9 Hz, Ru-*P*Ph$_3$). IR (Nujol, cm^{-1}): 1120 (s) (SO). HRMS m/z (%): 1547.1821 ([M – Cl]$^+$) calcd for $C_{76}H_{84}Cl_3GeN_2OP_3Ru_2S$ ([M – Cl]$^+$) 1547.1829.

Synthesis of 4a: 1 (140 mg, 0.31 mmol, 1 eq) and bis(1,5-cyclooctadiene) nickel (0) (125 mg, 0.31 mmol, 0.5 eq) were dissolved in toluene (3 mL). The mixture was stirred during 15 minutes at room temperature, the solvent was then removed under reduced pressure. Finally, the solid was washed with pentane (2x3 mL) to obtain a yellow solid (206 mg) in 89% yield. Crystallization from a solution of toluene at -24 °C gave pale yellow crystals suitable for X-ray diffraction analysis. ^{1}H NMR (300.18 MHz, C_6D_6, 25 °C): δ 0.51 (d, $^{3}J_{HH}$ = 6.3 Hz, 3H, CH(C$\boldsymbol{H}_3$)$_2$); 0.85 (d, $^{3}J_{HH}$ = 6.3 Hz, 3H, CH(C$\boldsymbol{H}_3$)$_2$); 1.10 (d, $^{3}J_{HH}$ = 6.3 Hz, 3H, CH(C$\boldsymbol{H}_3$)$_2$); 1.15 (s, 9H, C(C$\boldsymbol{H}_3$)$_3$); 1.28 (d, $^{3}J_{HH}$ = 6.3 Hz, 3H, CH(C$\boldsymbol{H}_3$)$_2$); 1.41 (s, 9H, C(C$\boldsymbol{H}_3$)$_3$); 1.98 (m, 1H, C$\boldsymbol{H}_2$-HC=CH); 2.18 (s, 3H, *p*-C$\boldsymbol{H}_3$); 2.34 (m, 2H, C$\boldsymbol{H}_2$-HC=CH); 2.65 (m, 4H, C$\boldsymbol{H}_2$-HC=CH); 3.22 (m, 1H, C$\boldsymbol{H}_2$-HC=CH); 3.98 (sept., $^{3}J_{HH}$ = 6.3 Hz, 2H, C$\boldsymbol{H}$(CH$_3$)$_2$); 4.54 (m, 1H, CH$_2$-$\boldsymbol{H}$C=CH); 4.85 (m, 1H, CH$_2$-$\boldsymbol{H}$C=CH); 5.09 (m, 1H, CH$_2$-$\boldsymbol{H}$C=CH); 5.41 (m, 1H, CH$_2$-$\boldsymbol{H}$C=CH); 6.99 (d, 1H, $^{3}J_{HH}$ = 8.2 Hz, C$\boldsymbol{H}_{Ar}$); 7.35 (s, 1H, C$\boldsymbol{H}_{Ar}$); 8.30 (d, 1H, $^{3}J_{HH}$ = 8.2 Hz, C$\boldsymbol{H}_{Ar}$).

Synthesis of 4b: 4a (80 mg, 0.13 mmol, 1 eq) in pressure tube was dissolved in C_6D_6 (0.5 mL) and $CO_{(gas)}$ atmosphere was added at room temperature (1.5 bar). The orange solution turn quickly bright yellow. Finally, the solvent was removed under reduced pressure and the solid was washed with pentane (3x4 mL) to obtain a yellow solid (75 mg) in 93% yield. Crystallization from toluene at -24 °C gave pale yellow crystals suitable for X-ray diffraction analysis. M.p. : 132 °C (decomposition); ^{1}H NMR (300.18 MHz, C_6D_6, 25 °C): δ 0.62 (d, $^{3}J_{HH}$ = 6.3 Hz, 3H, CH(C$\boldsymbol{H}_3$)$_2$); 0.94 (d, $^{3}J_{HH}$ = 6.3 Hz, 3H, CH(C$\boldsymbol{H}_3$)$_2$); 1.06 (s, 9H, C(C$\boldsymbol{H}_3$)$_3$); 1.16 (d, $^{3}J_{HH}$ = 6.3 Hz, 3H, CH(C$\boldsymbol{H}_3$)$_2$); 1.26 (s, 9H, C(C$\boldsymbol{H}_3$)$_3$); 1.33 (d, $^{3}J_{HH}$ = 6.3 Hz, 3H, CH(C$\boldsymbol{H}_3$)$_2$); 2.12 (s, 3H, *p*-C$\boldsymbol{H}_3$); 3.88 (sept., $^{3}J_{HH}$ = 6.3 Hz, 2H, C$\boldsymbol{H}$(CH$_3$)$_2$); 4.03 (m, 1H, CH$_2$-$\boldsymbol{H}$C=CH); 6.98 (d, 1H, $^{3}J_{HH}$ = 8.2 Hz, C$\boldsymbol{H}_{Ar}$); 7.63 (s, 1H, C$\boldsymbol{H}_{Ar}$); 7.92 (d, 1H, $^{3}J_{HH}$ = 8.2 Hz, C$\boldsymbol{H}_{Ar}$). ^{13}C{^{1}H} NMR (75.48 MHz, C_6D_6, 25 °C): δ 21.4 (p-$\boldsymbol{C}$H$_3$); 23.5 (O=SC($\boldsymbol{C}$H$_3$)$_3$); 23.8 (CH($\boldsymbol{C}$H$_3$)$_2$); 24.4 (CH($\boldsymbol{C}$H$_3$)$_2$); 26.3 (CH($\boldsymbol{C}$H$_3$)$_2$); 26.5 (CH($\boldsymbol{C}$H$_3$)$_2$); 29.1 (C($\boldsymbol{C}$H$_3$)$_3$); 39.6 ($\boldsymbol{C}$(CH$_3$)$_3$); 48.0 ($\boldsymbol{C}$H(CH$_3$)$_2$); 48.2 ($\boldsymbol{C}$H(CH$_3$)$_2$); 56.8 (O=S-$\boldsymbol{C}$(CH$_3$)$_3$); 126.6 ($\boldsymbol{C}_{Ar}$); 130.0 ($\boldsymbol{C}_{Ar}$); 133.0 ($\boldsymbol{C}_{Ar}$); 139.6 ($\boldsymbol{C}_{Ar/q}$); 145.7 ($\boldsymbol{C}_{Ar/q}$); 151.2 ($\boldsymbol{C}_{Ar/q}$); 173.6 (N−$\boldsymbol{C}$−N); 199.0 ($\boldsymbol{C}$O). IR (cm^{-1}) : 2059 (CO), 1982 (CO), 1027 (SO). HRMS m/z (%): 567.1246 ([M + 1 - CO]$^{+}$) calcd for $C_{24}H_{38}GeN_2O_4NiS$ ([M + 1]$^{+}$) 567.1241.

ASSOCIATED CONTENT

Supporting Information

The Supporting Information is available free of charge on the ACS Publications website.

Synthesis, characterizations, crystal structure refinements and computational investigations (PDF)

Accession Codes

‡ CCDC-1875989 (**2a**), CCDC-1875990 (**2b**), CCDC-1875991 (**3b**), CCDC-1875992 (**4a**) and CCDC-1875993 (**4b**) contain the supplementary crystallographic data for this paper. These data can be obtained free of charge from The Cambridge Crystallographic Data Centre via www.ccdc.cam.ac.uk/data_request/cif

AUTHOR INFORMATION

Corresponding Author

* **David Madec** – Laboratoire Hétérochimie Fondamentale et Appliquée (UMR 5069), Université de Toulouse, CNRS, 118, Route de Narbonne, 31062 Toulouse Cedex 09, France. orcid.org/0000-0002-5248-8947. E-mail: **madec@chimie.ups-tlse.fr**

Author

Nicolas Lentz – Laboratoire Hétérochimie Fondamentale et Appliquée (UMR 5069), Université de Toulouse, CNRS, 118, Route de Narbonne, 31062 Toulouse Cedex 09, France. orcid.org/0000-0003-1465-3099.

Cynthia Cuevas-Chavez – Laboratoire Hétérochimie Fondamentale et Appliquée (UMR 5069), Université de Toulouse, CNRS, 118, Route de Narbonne, 31062 Toulouse Cedex 09, France. orcid.org/0000-0001-5617-9773.

Sonia Mallet-Ladeira – Institut de Chimie de Toulouse (ICT, FR2599), 118, Route de Narbonne, 31062 Toulouse Cedex 09, France.

Jean-Marc Sotiropoulos – IPREM, UMR 5254 UPPA/CNRS – ECP Technopole Helioparc – 2, av. Pdt P. Angot – 64053 Pau cedex 09, France. orcid.org/0000-0001-9513-3639.

Antoine Baceiredo – Laboratoire Hétérochimie Fondamentale et Appliquée (UMR 5069), Université de Toulouse, CNRS, 118, Route de Narbonne, 31062 Toulouse Cedex 09, France. orcid.org/0000-0002-6428-9697.

Tsuyoshi Kato – Laboratoire Hétérochimie Fondamentale et Appliquée (UMR 5069), Université de Toulouse, CNRS, 118, Route de Narbonne, 31062 Toulouse Cedex 09, France. orcid.org/0000-0001-9003-4455.

Notes

The authors declare no competing financial interest.

ACKNOWLEDGMENT

This work was supported by the Centre National de la Recherche Scientifique (CNRS), the Université de Toulouse (UPS). N. L. is grateful to the Ministère de l'Enseignement Supérieur et de la Recherche for fellowships.

REFERENCES

1 Jeffrey, J. C.; Rauchfuss, T. B. Metal Complexes of Hemilabile Ligands. Reactivity and Structure of Dichlorobis(o-(diphenylphosphino)anisole)ruthenium(II). *Inorg. Chem.* **1979**, *18*, 2658-2666.

2 (a) Bader, A.; Lindner, E. Coordination Chemistry and Catalysis with Hemilabile Oxygen-phosphorus Ligands. *Coord. Chem. Rev.* **1991**, *108*, 27-110. (b) Slone, C. S.; Weinberger, D. A.; Mirkin, C. A. The Transition Metal Coordination Chemistry of Hemilabile Ligands. *Prog. Inorg. Chem.* **1999**, *48*, 233-350. (c) Braunstein, P.; Naud, F. Hemilability of Hybrid Ligands and the Coordination Chemistry of Oxazoline-Based Systems. *Angew. Chem. Int. Ed.* **2001**, *40*, 680-699. (d) Bassetti, M. Kinetic Evaluation of Ligand Hemilability in Transition Metal Complexes. *Eur. J. Inorg. Chem.* **2006**, 4473-4482. (e) Weng, Z.; Teo, S.; Hor, T. S. A. Metal Unsaturation and Ligand Hemilability in Suzuki Coupling. *Acc. Chem. Res.* **2007**, *40*, 676-684. (f) Oliveri, C. G.; Ulmann, P. A.; Wiester, M. J.; Mirkin, C. A. Heteroligated Supramolecular Coordination Complexes Formed via the Halide-Induced Ligand Rearrangement Reaction. *Acc. Chem. Res.* **2008**, *41*, 1618-1629. (g) Adams, G. M.; Weller, A. S. POP-type ligands: Variable Coordination and Hemilabile Behavior. *Coord. Chem. Rev*. **2018**, *355*, 150-172.

3 (a) Petz, W. Transition-Metal Complexes with Derivatives of Divalent Silicon, Germanium, Tin, and Lead as Ligands. *Chem. Rev*. **1986**, *86*, 1019-1047. (b) Lappert, M. F.; Rowe, R. S. The Role

of Group 14 Element Carbene Analogues in Transition Metal Chemistry. *Coord. Chem. Rev.* **1990**, *100*, 267-292. (c) Leung, W.-P.; Kan, K.-W.; Chong, K.-H. Reactions of Some Organogermanium(II) Chlorides. *Coord. Chem. Rev.* **2007**, *251*, 2253-2265. (d) Nagendran, S.; Sen, S. S.; Roesky, H. W.; Koley, D.; Grubmüller, H.; Pal, A.; Herbst-Irmer, R. RGe(I)Ge(I)R Compound (R = PhC(N*t*Bu)$_2$) with a Ge−Ge Single Bond and a Comparison with the Gauche Conformation of Hydrazine. *Organometallics* **2008**, *27*, 5459-5463. (e) Zabula, A. V.; Hahn, F. E. Mono- and Bidentate Benzannulated N- Heterocyclic Germylenes, Stannylenes and Plumbylenes. *Eur. J. Inorg. Chem.* **2008**, 5165-5179. (f) Mandal, S. K.; Roesky, H. W. Interstellar Molecules: Guides for New Chemistry. *Chem. Commun.* **2010**, 6016-6041. (g) Panday, K. K.; Power, P. P. Nature of M–E Bonds in Metallosilylenes, -Germylenes, -Stannylenes, and -Plumbylenes [(η5-C_5H_5)(Me_3P)$(H)_2$M(EPh)] (M = Fe, Ru, Os; E = Si, Ge, Sn, Pb). *Organometallics* **2011**, *30*, 3353-3361. (h) Baumgartner, J.; Marschner, C. Coordination of Non-Stabilized Germylenes, Stannylenes, and Plumbylenes to Transition Metals. *Rev. Inorg. Chem.* **2014**, *34*, 119-152. (i) Portnyagin, I. A.; Nechaev, M. S. Germylene and Stannylene ($Me_2NCH_2CH_2O)_2$E as Strong σ-Donor Ligands for Transition Metal Complexes [ML$(CO)_n$] (E = Ge, Sn; M = Cr, Mo, W, n = 4 or 5; M = Fe, n = 4). Synthesis, Spectroscopic and Theoretical Study. *J. Organomet. Chem.*, **2009**, *694*, 3149-3153. (j) Benedek, Z.; Szilvási, T. Theoretical Assessment of Low-Valent Germanium Compounds as Transition Metal Ligands: Can They Be Better than Phosphines or NHCs? *Organometallics* **2017**, *36*, 1591-1600. (k) Matioszek, D.; Katir, N.; Saffon, N.; Castel A. Halogermanium(II) Complexes Having Phenylamidinate as Supporting Ligands: Syntheses, Characterizations, and Reactivities. *Organometallics* **2010**, *29*, 3039-3046. (l) El Ezzi, M.; Kocsor, T.-G.; D'Accriscio, F.; Madec, D.; Mallet-Ladeira, S.; Castel, A. Iron Complexes with Stabilized Germylenes: Syntheses and Characterizations. *Organometallics* **2015**, *34*, 571-576. (m) Álvarez-Rodríguez, L.; Cabeza, J. A.; García-Álvarez, P.; Polo, D. The Transition-Metal Chemistry of Amidinatosilylenes, -Germylenes and –Stannylenes. *Coord. Chem. Rev.* **2015**, *300*, 1-28. (n) Chlupatý, T.; Růžička, A. Hybrid Amidinates and Guanidinates of Main Group Metals. *Coord. Chem. Rev.* **2016**, *314*, 103-113.

4 (a) Brück, A.; Gallego, D.; Wang, W.; Irran, E.; Driess, M.; Harwig, J. F. Pushing the σ- Donor Strength in Iridium Pincer Complexes: Bis(silylene) and Bis(germylene) Ligands Are Stronger Donors than Bis(phosphorus(III)) Ligands. *Angew. Chem. Int. Ed.* **2012**, *51*, 11478-11482. (b) Wang, W.; Inoue, S.; Enthaler, S.; Driess, M. Bis(silylenyl)- and Bis(germylenyl)- Substituted Ferrocenes: Synthesis, Structure, and Catalytic Applications of Bidentate Silicon(II)–Cobalt Complexes. *Angew. Chem. Int. Ed.* **2012**, *51*, 6167-6171. (c) Gallego, D.; Brück, A.; Irran, E.; Meier, F.; Kaupp, M.; Driess, M.; Harwig, J. F. From Bis(silylene) and Bis(germylene) Pincer-Type Nickel(II) Complexes to Isolable Intermediates of the Nickel-Catalyzed Sonogashira Cross-Coupling Reaction. *J. Am. Chem. Soc.* **2013**, *135*, 15617-15626. (d) Gallego, D.; Inoue, S.; Blom, B.; Driess, M. Highly Electron-Rich Pincer-Type Iron Complexes Bearing Innocent Bis(metallylene)pyridine Ligands: Syntheses, Structures, and Catalytic Activity. *Organometallics* **2014**, *33*, 6885-6897. (e) Álvarez-Rodríguez, L.; Cabeza, J. A.; Fernández-Colinas, J. M.; García-Álvarez, P.; Polo, D. Amidinatogermylene Metal Complexes as Homogeneous Catalysts in Alcoholic Media. *Organometallics* **2016**, *35*, 2516-2523. (f) Sharma, M. K.; Singh, D.; Mahawar, P.; Yadav, R.; Nagendran, S. Catalytic Cyanosilylation Using Germylene Stabilized Platinum(II) Dicyanide. *Dalton Trans.* **2018**, *47*, 5943-5947.

5 Lentz, N.; Mallet-Ladeira, S.; Baceiredo, A.; Kato, T.; Madec, D. Germylene–Sulfoxide as a Potential Hemilabile Ligand: Application in Coordination Chemistry. *Dalton Trans.*, **2018**, *47*, 15751-15756.

6 (a) Cotton, F. A.; Francis, R.; Horrocks, W. D. Sulfoxides as ligands. II. The Infrared Spectra of Some Dimethyl Sulfoxide Complexes. *J. Phys. Chem.* **1960**, *64*, 1534-1536. (b) Davies, A. R.; Einstein, F. W. B.; Farrell, N. P.; James, B. R.; McMillan, R. S. Synthesis, Properties, and X-ray Structural Characterization of the Hexakis(dimethyl sulfoxide)ruthenium(II) cation. *Inorg. Chem.* **1978**, *17*, 1965-1969.

7 (a) Jones, C.; Rose, R. P.; Stasch, A. Synthesis, Characterisation and Reactivity of Germanium(II) Amidinate and Guanidinate Complexes. *Dalton Trans.* **2008**, *21*, 2871-2878. (b) Matioszek, D.; Katir, N.; Saffon, N.; Castel, A. Halogermanium(II) Complexes Having Phenylamidinate as Supporting Ligands: Syntheses, Characterizations, and Reactivities. *Organometallics* **2010**, *29*, 3039-3046. (c) Matioszek, D.; Kocsor, T.-G.; Castel, A.; Nemes, G.; Escudié, J.; Saffon, N. Phosphaalkenyl Germylenes and their Gold, Tungsten and Molybdenum Complexes. *Chem. Commun.* **2012**, *48*, 3629-3631. (d) Tokitoh, N.; Manmaru, K.; Okazaki, R. Synthesis and Crystal Structure of the First Base-Free Diarylgermylene-Transition Metal Mononuclear Complexes. *Organometallics* **1994**, *13*, 167-171. (e) Zabula, A. V.; Hahn, F. E.; Pape, T.; Hepp, A. Preparation and Coordination Chemistry of Bidentate Benzimidazoline-2-germylenes. *Organometallics* **2007**, *26*, 1972-1980. (f) Kühl, O.; Lönnecke, P.; Heinicke, J. Formation and Structure of fac-[Mo$(CO)_3$(C_2H_2[N(CH_2But)]$_2$Ge)$_3$]: The First Structurally Characterized Group 6 Transition Metal Complex of an Unsaturated Diaminogermylene. *Inorg. Chem.* **2003**, *42*, 2836-2838. (g) Ullah, F.; Kühl, O.; Bajor, G.; Veszprémi, T.; Jones, P. G.; Heinicke, J. Transition Metal Complexes of N- Heterocyclic Germylenes. *Eur. J. Inorg. Chem.* **2009**, 221-229.

8 (a) Cabeza, J. A.; Fernández-Colinas, J. M.; García-Álvarez, P.; Polo, D. Steric Effects in the Reactions of Amidinate Germylenes with Ruthenium Carbonyl: Isolation of a Coordinatively Unsaturated Diruthenium(0) Derivative. *RSC Adv.* **2014**, *4*, 31503-31506. (b) Álvarez-Rodríguez, L.; Cabeza, J. A.; García-Álvarez, P.; Pérez-Carreño, E. Ruthenium Carbene Complexes Analogous to Grubbs-I Catalysts Featuring Germylenes as Ancillary Ligands. *Organometallics* **2018**, *37*, 3399-3406. (c) Brugos, J.; Cabeza, J. A.; García-Álvarez, P.; Pérez-Carreño, E. From a PGeP Pincer-Type Germylene to Metal Complexes Featuring Chelating (Ir) and Tripodal (Ir) PGeP Germyl and Bridging (Mn_2) and Chelating (Ru) PGeP Germylene Ligands. *Organometallics* **2018**, *37*, 1507-1514. (d) Hayes, P. G.; Waterman, R.; Glaser, P. B.; Don Tilley, T. Synthesis, Structure, and Reactivity of Neutral Hydrogen-Substituted Ruthenium Silylene and Germylene Complexes. *Organometallics* **2009**, *28*, 5082-5089.

9 (a) Goicoechea, J. M.; Mahon, M. F.; Whittlesey, M. K.; Kumar, P. G. A.; Pregosin, P. S. Mononuclear and Dinuclear Complexes with a [Ru(*t*Bu_2PCH_2CH_2P*t*Bu_2)(CO)] Core. *Dalton Trans.* **2005**, 588-597. (b) Hargreaves, M. D.; Mahon, M. F.; Whittlesey, M. K. Substitution Reactions of [Ru(dppe)$(CO)(H_2O)_3$][OTf]$_2$. *Inorg. Chem.* **2002**, *41*, 3137-3145. (c) Flowers, S. E.; Johnson, M. C.; Pitre, B. Z.; Cossairt, B. M. Synthetic Routes to a Coordinatively Unsaturated Ruthenium Complex Supported by a Tripodal, Protic Bis(N-Heterocyclic Carbene) Phosphine Ligand. *Dalton Trans.* **2018**, *47*, 1276-1283.

10 (a) Tanase, T.; Aiko, T.; Yamamoto Y. A Diruthenium(II) Complex Containing an Unprecedented Bridging S,O-Bidentate Dimethyl Sulfoxide Ligand. *Chem. Commun.* **1996**, 2341-2342. (b) Geremia, S.; Mestroni, S.; Calligaris, M.; Alessio, E. The First Example of a Double Bridged Diruthenium(II) Complex Containing the Rare Bridging S,O Bidentate Dimethyl Sulfoxide Ligand which Defines a Stable Ru–Cl–Ru–S–O Five-Membered Ring. *Dalton Trans.* **1998**, 2447-2448. (c) Nakatani, E.; Takai, Y.; Kurosawa, H. Coordination Behavior of some Bridge Ligands Having S–O Bond Bound to Four-Membered ring Unit (Ru_2O_2) of Dinuclear Areneruthenium Complexes. *J. Organomet. Chem.* **2007**, *692*, 278-285. (d) de Paula, Q. A.; dos Santos, S.; Ellena, J.; Castellano, E. E.; Batista, A. A. Spectroscopic Investigation on the Formation of a Dinuclear Me_2SO–Ru_2-Mercaptopyridine Bridged Complex: [Ru_2Cl_3(μ-pyS)(μ-dmso)(dmso)$_4$] · $2H_2O$. *J. Chem. Cryst.* **2009**, *39*, 519-524. (e) Calligaris, M. Structure and Bonding in Metal Sulfoxide Complexes: An Update. *Coord. Chem. Rev.* **2004**, *248*, 351-375.

11 (a) Herrmann, W. A.; Denk, M.; Behm, J.; Scherer, W.; Klingan, F.-R.; Bock, H.; Solouki, B.; Wagner, M. Stable Cyclic Germanediyls ("Cyclogermylenes"): Synthesis, Structure, Metal Complexes, and Thermolyses. *Angew. Chem. Int. Ed.* **1992**, *31*, 1485-1488. (b) Veith, M.; Stahl, L. Novel Insertions of Carbene Homo-

logues into Metal- η5−Cp Bonds: Sandwich Complexes with Ge_2Ni and Sn_2Ni Cores. *Angew. Chem. Int. Ed.* **1993**, *32*, 106-107. (c) Litz, K. E.; Bender, J. E.; Kampf, J. W.; Holl, M. M. B. Transition Metal Germylene Complexes as Hydrogenation Catalysts: The Synthesis of a Rare Bis(amino)germane. *Angew. Chem. Int. Ed*. **1997**, *36*, 496-498. (d) Grenz, M.; Hahn, E.; du Mont, W.-W.; Pickardt, J. Novel Structures Containing Germanium(II): Germanocene Dimeric Tricarbonyl(di- tert- butoxygermylene)nickel(0). *Angew. Chem. Int. Ed.* **1984**, *23*, 61-63. (e) Watanabe, T.; Kasai, Y.; Tobita, H. A Nickel Complex Containing a Pyramidalized, Ambiphilic Pincer Germylene Ligand. *Chem. Eur. J.*, **2019**, *25*, 13491-13495. (f) Gendy, C.; Mansikkamaki, A.; Valjus, J.; Heidebrecht, J.; Hui, P. C.-Y.; Bernard, G. M.; Tuononen, H. M.; Wasylishen, R. E.; Michaelis, V. K.; Roesler, R. Nickel as a Lewis Base in a T- Shaped Nickel(0) Germylene Complex Incorporating a Flexible Bis(NHC) Ligand. *Angew. Chem. Int. Ed.* **2019**, *58*, 154-158. (g) Cabeza, J. A. ; García-Álvarez, P. ; Laglera-Gándara, C. J.; Pérez-Carreño, E. Phosphane-Functionalized Heavier Tetrylenes: Synthesis of Silylene- and Germylene-Decorated Phosphanes and their Reactions with Group 10 Metal Complexes. *Dalton Trans.* **2020**, *49*, 8331-8339.

12 Suess, D. L. M.; Peters, J. C. Late-Metal Diphosphinosulfinyl $S(O)P_2$ Pincer-type Complexes. *Organometallics* **2012**, *31*, 5213-5222.

13 (a) Tolman, C. A. Steric Effects of Phosphorus Ligands in Organometallic Chemistry and Homogeneous Catalysis. *Chem.Rev.* **1977**, *77*, 313-348. (b) Nelson, D. J.; Nolan, S. P. Quantifying and Understanding the Electronic Properties of N-Heterocyclic Carbenes. *Chem. Soc. Rev.* **2013**, *42*, 6723-6753.

14 G. M. Sheldrick. SHELXT – Integrated space-group and crystal-structure determination. *Acta Cryst. Sect. A*, **2015**, A71, 3–8.

15 G. M. Sheldrick. SHELXT – Integrated space-group and crystal-structure determination. *Acta Cryst. Sect. C*, **2015**, C71, 3–8.

16 P. van der Sluis and A. L. Spek. BYPASS: an effective method for the refinement of crystal structures containing disordered solvent regions. *Acta Cryst., Sect. A*, **1990**, 46, 194-201.

17 sGaussian 09, Revision D.01, M. J. Frisch, G. W. Trucks, H. B. Schlegel, G. E. Scuseria, M. A. Robb, J. R. Cheeseman, G. Scalmani, V. Barone, B. Mennucci, G. A. Petersson, H. Nakatsuji, M. Caricato, X. Li, H. P. Hratchian, A. F. Izmaylov, J. Bloino, G. Zheng, J. L. Sonnenberg, M. Hada, M. Ehara, K. Toyota, R. Fukuda, J. Hasegawa, M. Ishida, T. Nakajima, Y. Honda, O. Kitao, H. Nakai, T. Vreven, J. A. Montgomery, Jr., J. E. Peralta, F. Ogliaro, M. Bearpark, J. J. Heyd, E. Brothers, K. N. Kudin, V. N. Staroverov, T. Keith, R. Kobayashi, J. Normand, K. Raghavachari, A. Rendell, J. C. Burant, S. S. Iyengar, J. Tomasi, M. Cossi, N. Rega, J. M. Millam, M. Klene, J. E. Knox, J. B. Cross, V. Bakken, C. Adamo, J. Jaramillo, R. Gomperts, R. E. Stratmann, O. Yazyev, A. J. Austin, R. Cammi, C. Pomelli, J. W. Ochterski, R. L. Martin, K. Morokuma, V. G. Zakrzewski, G. A. Voth, P. Salvador, J. J. Dannenberg, S. Dapprich, A. D. Daniels, O. Farkas, J. B. Foresman, J. V. Ortiz, J. Cioslowski, and D. J. Fox, Gaussian, Inc., Wallingford CT, 2013.

18 D. Andrae, U. Häußermann, M. Dolg, H. Stoll, H. Preuß. Energy-adjustedab initio pseudopotentials for the second and third row transition elements. Theor. Chim. Acta 1990, 77, 123–141.

19. A. W. Ehlers, M. Böhme, S. Dapprich, A. Gobbi, A. Höllwarth, V. Jonas, K. F. Köhler, R. Stegmann, A. Veldkamp, G. Frenking. A set of f-polarization functions for pseudo-potential basis sets of the transition metals Sc-Cu, Y-Ag and La-Au. Chem. Phys. Lett. 1993, 208, 111–114.